This is the peer reviewed version of Hoult, N.A. and Lees, J.M. (2009) "Modelling of an Unbonded CFRP Strap Shear Retrofitting System for RC Beams" ASCE Journal of Composites for Construction, v. 13 (4) pp. 292-301 which has been published on http://dx.doi.org/10.1061/(ASCE)CC.1943-5614.0000013

Modelling of an Unbonded CFRP Strap Shear Retrofitting System for RC Beams

Neil A. Houlti[1] and Janet M. Lees[2]

Abstract

A retrofitting technique has been developed that uses carbon fiber reinforced polymer (CFRP) straps to increase the shear capacity of reinforced concrete beams. The vertical straps are not bonded to the beam but are instead anchored against the beam which makes this technique potentially more effective than bonded FRP retrofitting techniques. However it also means that models for bonded FRPs are not appropriate for use with the straps. Instead a model based on a shear friction approach has been developed where the strain in the straps is calculated based on a term that accounts for the effects of prestress and additional strain in the strap due to shear crack opening. The model can either consider the shear reinforcement to be smeared along the length of the beam or discrete elements. The 'smeared' model was checked against an experimental database consisting of rectangular, T- and deep beams both in terms of predicted capacity and predicted strain in the straps. Overall the 'smeared' model predicted the capacity of the specimens and, with some adjustments, the strains quite accurately. There were however cases when it was more appropriate to use the 'discrete' model such as when the transverse reinforcement ratio was low or when the transverse reinforcement spacing was high. Further experimental data is required to fully validate the models and to determine appropriate limits on the use of the 'smeared' model and the 'discrete' model. However the initial results are promising.

CE Database Subject Headings: Shear; Concrete, prestressed; Fiber reinforced polymers; Concrete beams.

[1] Research Associate, Dept. of Engineering, Univ. of Cambridge, Trumpington St., Cambridge, CB2 1PZ, UK. E-mail: nah25@cam.ac.uk
[2] University Senior Lecturer, Dept. of Engineering, Univ. of Cambridge, Trumpington St., Cambridge, CB2 1PZ, UK. E-mail: jmL2@cam.ac.uk

Introduction

Globally the need to both maintain and expand civil infrastructure is increasingly at odds with decreasing government budgets. In the case of existing Reinforced Concrete (RC) structures, many have insufficient shear capacity due to increased loading requirements, designs based on earlier less-conservative codes, corrosion of the transverse reinforcing steel or increased flexural capacity as a result of retrofitting.

Much of the research relating to the shear retrofitting of RC beams using FRPs has investigated bonded FRP fabrics or sheets. The capacity enhancement provided by bonded solutions is often limited by how effectively force can be transferred to the FRP, which is a function of the bond between the concrete and the FRP as well as the FRP development length. Some of these issues can be overcome by fully wrapping beams (e.g. Melo *et al*. 2003) but such installations may not be practical in typical slab-on-beam type construction.

The current work focuses on a FRP retrofitting technique that uses *unbonded* Carbon FRP (CFRP) straps. This system, first proposed by Winistoefer (1999), uses CFRP straps wrapped around the cross section of a beam as illustrated in **Fig. 1**. The straps are installed at discrete locations along the length of the beam. The number of loops in the strap can be varied depending on the shear capacity required as only the outermost layer must be connected to the next layer by welding the thermoplastic matrices together in order to form a closed loop. When load is applied to the strap, the inner loops tighten against the closed outer loop allowing each layer to take approximately the same amount of tension. These straps can also be prestressed with an initial force which can have a beneficial effect on the capacity of some specimens as will be discussed later.

A number of models exist for calculating the shear enhancement provided by FRPs (Berset 1992, Deniaud and Cheng 2001 and 2003, Khalifa *et al.* 1998) but these models are intended for passive *bonded* continuous FRP sheets. In contrast, the CFRP straps are unbonded, prestressed (if required by the design), and installed at discrete locations. Each

of these characteristics leads to challenges when developing a model for calculating the retrofitted strength of the structure. As the straps are unbonded, the strain in the strap is not controlled by localized behaviour in the region of a crack as it would be for a bonded system. Rather strap strain is a function of the strain due to the initial prestress, $\varepsilon_{prestress}$, plus an additional strain component at the location of the strap, ε_{cr}, which is calculated by summing the crack openings over the height of the strap and dividing the total displacement by the unbonded length of the strap. As the straps are discrete elements, failure planes can potentially form between individual straps. The impact of the strap strain in terms of creating a clamping stress across the shear cracks is a further consideration. Research (Walraven 1981) has shown that increasing clamping action reduces the crack widths and thus enhances the concrete contribution to the shear capacity.

As with all FRPs, the brittle-elastic material behaviour leads to two further complications. First the strain in the straps must be accurately known in order to calculate their contribution to the overall shear capacity. Second, because the material is brittle the assumption of plasticity cannot be made as it is with steel transverse reinforcement. In fact, if the FRP strain is not predicted correctly then strap rupture may be missed, which could lead to overestimates of capacity or incorrect predictions of the failure mode.

A review of a number of existing shear theories (Hoult and Lees 2007) was conducted to determine how easily a given model could be adapted to incorporate CFRP straps and also the ability of the model to predict the ultimate capacities of CFRP strap strengthened beams. As a result of this review, a model proposed by Loov (1998) based on a shear friction approach was identified as having promise and will be the focus of the work reported here. As mentioned previously, it is critical to know the strain in the CFRP straps due to crack openings, ε_{cr}. However, the Loov model as originally developed does not have an approach for the calculation of crack widths and so a formulation for calculating crack widths proposed by Vecchio and Collins (1986) will be introduced. Furthermore, the Loov model is for rectangular specimens and so an extension of the model by Deniaud and Cheng (2003) that allows it to be used for T-beams will also be

presented so that the model can be applied to a more extensive experimental database. Deniaud and Cheng developed their model for use with FRP retrofitted beams, however, the FRP contribution was intended for bonded systems and so will not be presented here.

By combining the work of Loov, Deniaud and Cheng, and Vecchio and Collins, this paper will introduce a shear friction formulation that is applicable to both rectangular and T-beam sections and will highlight the modifications required to incorporate the CFRP straps. The importance of the clamping action created by the straps and the implications of their discrete nature are investigated to determine whether simplifying assumptions can be incorporated without an undue loss of accuracy. To confirm the generality of the approach, the predictions are compared with a database of experimental specimens including rectangular, T- and deep beams.

Shear Friction Modelling and Design Approaches

The concept of shear friction assumes that, after concrete cracks, shear stresses can still be carried across the crack. This is due to the fact that cracks in concrete are never completely smooth and as one side of the crack moves relative to the other the rough crack faces wedge against one another. Numerous different shear friction models which relate the shear stress, *v*, that can be carried across a crack to the clamping stress perpendicular to the crack, σ, are available in the literature (e.g. Walraven 1981, Walraven *et al*. 1987). This ability of concrete to carry shear across a crack is reflected, to a greater or lesser extent, in a number of design approaches to determine the ultimate shear capacity of reinforced concrete beams. Of particular interest in the current work is a shear friction approach developed by Loov for rectangular beams which has been extended for use with T-beams.

Loov Shear Friction Approach Applied to Rectangular Beams

Loov (1998) proposed that the relationship between σ and *v* is a function of the concrete compressive strength, $f_c^{'}$ and a parameter, *k* where:

$$v = k\sqrt{\sigma f_c'} \quad (1)$$

The parameter k is analogous to a coefficient of friction and was initially proposed to be 0.6 by Kumaraguru (1992) based on an analysis of push-off tests conducted by Walraven *et al*. (1987), Hofbeck *et al*. (1969) and Mattock and Hawkins (1972). Loov and Peng (1998) suggested that k also depends on the concrete strength:

$$k = 2.1\left(f_c'\right)^{-0.4} \leq 0.5 \quad (2)$$

where f_c' is in MPa.

Loov proposes that the crack shear and clamping stresses can be considered in an average sense and represented as resultant forces acting on a structure subjected to applied loads as illustrated by the combination of forces shown in **Fig. 2(a).** This representation assumes a crack has formed at an angle θ and the force in the longitudinal reinforcement, T, the total force in the transverse reinforcement, ΣT_v, the shear friction force S (the resultant of the shear stress, v, in equation 1) and associated clamping force R (the resultant of the clamping stress, σ, in equation 1) all act to resist the total applied shear force, V_n, axial force, N (where present) and applied moment M. In this model the clamping force, R, is a function of the force in the longitudinal reinforcement, T, and the crack angle, θ. The crack angle is also affected by the total transverse reinforcement contribution, ΣT_v, which then indirectly affects the clamping force as will be discussed later. It should also be noted that any dowel action contributed by the reinforcement has been neglected. By resolving the forces in **Fig 2(a)** in the direction parallel and perpendicular to the crack and incorporating a simplifying assumption for the force T, the nominal ultimate shear strength, V_n, of a rectangular RC beam with steel stirrups with no axial load can be calculated as (for further details see Loov (1998)):

$$V_n = 0.25k^2 f_c' b_w h \tan\theta + T_v n_v \quad (3)$$

Where b_w is the width of the web in mm, h is the total height of the section in mm, T_v is the force in Newtons in an individual transverse reinforcement element and n_v is the number of transverse reinforcement elements crossed by the crack. In equation (3), all safety factors have been set to unity in order to check the accuracy of the model.

The internal transverse steel reinforcement is treated as a series of discrete elements and equation (3) is evaluated by considering potential failure planes as illustrated in **Fig. 2(b)**. If the crack crosses an internal steel link, the stirrup is assumed to yield. Calculating the minimum shear strength then becomes an optimization problem. The concrete contribution is minimized when the shear crack angle is a minimum (i.e. Plane 3 in **Fig. 2(b)**) whereas to minimize the transverse reinforcement contribution the plane that crosses the fewest reinforcement elements is critical (i.e. Plane 1 in **Fig. 2(b)**). Loov (1998) suggests limits on V_n (since for higher values of θ, V_n would approach infinity) which depend on the concrete strength.

Extensions to the Shear Friction Approach Required for T-beams

Many existing structures are not rectangular and the versatility to represent slab-on-beam or T-beam type structures in a shear design approach is an advantage. To extend the Loov approach for use with T-beams, where the web and flange areas, shear resistance and crack angles potentially differ, Deniaud and Cheng (2003) modified Equation 3 as follows:

$$V_n = 0.25 f_c^{'} \left(k_w^2 A_{cw} \tan\theta_w + k_f^2 A_{cf} \tan\theta_f \right) + T_v n_v \qquad (4)$$

where A_{cw} is the area of the web contributing to the shear force, θ_w is the crack angle in the web, A_{cf} is the area of the flange contributing to shear friction and θ_f is the crack angle in the flange. The effective concrete areas A_{cw} and A_{cf} as proposed by Tozser and Loov (1999) are illustrated in **Fig. 3.** To determine the appropriate values of k_w and k_f, Deniaud and Cheng extrapolated the research of Kumaraguru (1992) who suggested that k = 0.6

was appropriate for beams because it was conservative for the uncracked regions and unconservative for the cracked regions. They therefore suggest a value of 0.5 for k_w in the cracked web and 0.7 for k_f in the largely uncracked flange. The critical values of θ_w and θ_f are determined by considering different failure planes and finding the minimum value of V_n.

Vecchio and Collins Crack Width Model

As mentioned previously, in order to estimate the strain in the CFRP straps due to crack opening, ε_{cr}, an estimate of the shear crack width, w, will be required. Unfortunately the Loov shear friction model represented in Equation 1 does not explicitly calculate the crack width. This limitation could be overcome if it were possible to associate the applied shear stress with a given crack opening while maintaining the integrity of the overall design approach. Duthinth (1999) summarized a number of possible shear friction models and found that most shear friction models are calibrated against the same push-off tests, namely those performed by Walraven (1981). The reported models generally showed a reasonable agreement for a crack width of 0.5 mm and applied stresses less than about 8-10 MPa but for higher stresses and larger crack widths the model predictions diverged.

Equation 1 has also been calibrated against Walraven's push-off tests (Kumaraguru 1992) which would imply a certain compatibility with other shear friction models, some of which include a crack width term, that have been calibrated against similar push-off test results. One example of such a model is that of Vecchio and Collins (1986). In their model, the crack width, w, can be estimated using equations 5 and 6:

$$w = \frac{\left(\frac{\sqrt{f_c'}}{v_{cimax}} - 0.31\right)\left(a_{agg} + 16\right)}{24} \tag{5}$$

$$v = 0.18 v_{cimax} + 1.64\sigma - 0.82\frac{\sigma^2}{v_{cimax}} \tag{6}$$

where $f_c^{'}$, v, v_{cimax} and σ are in MPa while w and the maximum aggregate diameter, $a_{agg,}$ are in mm. Vecchio and Collins make a distinction between localized stress concentrations, $v_{ci\max}$, where aggregates come into contact along the crack face and the average stress that is transferred across the crack face v.

Incorporation of the CFRP Straps

The form of equations 3 and 4 are such that additional CFRP reinforcement can be included as an additional term. However, two modifications to the shear friction formulations were developed in the current work in order to include the unbonded prestressed CFRP strap reinforcement.

The first modification was to develop a 'smeared' version of the Loov (1998) and Deniaud and Cheng (2003) models. This was done in order to reduce the complexity of the analysis. In the original Loov formulation, discrete transverse reinforcement elements are considered to determine the critical crack angle. However in a region of constant shear when the CFRP straps are included at a potentially different spacing to the internal steel reinforcement the number of failure plane locations and angles, and corresponding iterations required to calculate the critical failure plane, increase dramatically. By using a 'smeared' approach the designer need only vary the crack angle (and not the location of the crack angle along the beam) to obtain the optimum solution. However, there are areas where a smeared approach may not be appropriate as will be discussed later and so the discrete version of the model will also be presented. The second modification involves the inclusion of a term, F_{FRP}, to account for the addition of the CFRP straps.

The resulting T-beam formulations with these two new developments for members with internal stirrups and external prestressed CFRP straps will be highlighted in the following. A similar approach was used for the rectangular beam predictions with the exception that only 'web' terms were considered and equation 2 was used to calculate *k*. The shear capacity of a T-beam with external CFRP reinforcement can be determined as:

$$V_n = 0.25 f_c' \left(k_w^2 A_{cw} \tan\theta_w + k_f^2 A_{cf} \tan\theta_f \right) + F_v + F_{FRP} \quad \text{(N)} \qquad (7)$$

where F_v is the contribution from the internal transverse steel reinforcement and F_{FRP} is the contribution of the CFRP straps. When a 'discrete' version of the model is considered (i.e. the optimum value of nominal shear force, V_n, is found by checking all the potential failure planes along the full length of the beam) then the terms F_v and F_{FRP} can be determined using equations 8a and 8b:

$$F_v = n_{vweb} A_{sv} f_{yv} + n_{vflange} A_{sv} f_{yv} \qquad \text{(N)} \qquad (8a)$$

$$F_{FRP} = n_{FRPweb} A_{FRP} E_{FRP} \left(\varepsilon_{prestress} + \varepsilon_{cr} \right) + n_{FRPflange} A_{FRP} E_{FRP} (\varepsilon_{prestress}) \quad \text{(N)} \qquad (8b)$$

where the area of the internal transverse reinforcement, A_{sv}, and the area of the CFRP straps, A_{FRP}, are both taken in mm^2. The yield strength of the internal transverse reinforcement, f_{yv}, and the modulus of elasticity for the CFRP, E_{FRP}, are both given in MPa. The number of internal transverse reinforcement elements crossing the web, n_{vweb}, and the flange, $n_{vflange}$, as well as the number of CFRP straps crossing the crack in the web, n_{FRPweb}, and the flange, $n_{vflange}$, are also required.

The analogous transverse reinforcement contributions for the 'smeared' model are:

$$F_v = \rho_v b_w L_{vweb} f_{yv} + \rho_v b_w L_{vflange} f_{yv} \quad \text{(N)} \qquad (9a)$$

$$F_{FRP} = F_{FRPweb} + F_{FRPflange} \qquad \text{(N)} \qquad (9b)$$

where $\rho_v = \dfrac{A_{sv}}{s_v b_w}$

s_v = spacing of internal transverse reinforcement (mm)

$L_{vweb} = (h - h_f - c_v)/\tan\theta_w$ (mm)

$L_{vflange} = (h_f - c_v)/\tan\theta_f$ (mm)

$$F_{FRPweb} = \rho_{FRP} b_w L_{FRPweb} E_{FRP} \left(\varepsilon_{prestress} + \varepsilon_{cr} \right)$$

$$L_{FRPweb} = (h - h_f - c_{FRPB}) / \tan\theta_w \text{ (mm)}$$

$$F_{FRPflange} = \rho_{FRP} b_w L_{FRPflange} E_{FRP} \left(\varepsilon_{prestress} \right) \text{ (N)}$$

$$L_{FRPflange} = (h_f - c_{FRPT}) / \tan\theta_f \text{ (mm)}$$

Equations 9a and 9b require the full height of the section, h, the height of the flange, h_f, the clear vertical cover to the internal transverse steel reinforcement, c_v, the cover to the CFRP strap on the bottom of the beam, c_{FRPB}, and the cover to the CFRP strap on top of the beam, c_{FRPT}, which are also illustrated in **Fig. 3** as inputs. Note that the cover to the top surface of the strap is taken into account to reflect cases where the strap does not extend to the top of the beam (see **Fig. 3**), which is the case when the straps are installed when access to the beam is from the underside only as discussed by Hoult and Lees (*in press*).

In equations 8a and 9a, any transverse steel reinforcement crossed by a crack is assumed to yield. In equations 8b and 9b, the prestressed CFRP straps are brittle elastic elements and so the strap force in the web is a function of both the initial prestrain and the crack opening strain. However, the CFRP strap contribution in the flange is considered to be dependant only on the level of prestress in the strap. This is because if one assumes that k_f is equal to 0.7 because the flange is largely uncracked (Deniaud and Cheng 2003), it is then unreasonable to base the CFRP strap contribution on a crack width strain term. Thus the CFRP strap contribution to the flange capacity is based on the strain due to prestress only.

To determine the crack opening strain, Loov's shear friction model (equation 1) was calibrated with Vecchio and Collins model (equations 5 and 6). The relationship between varying values of clamping stress, σ, and shear stress, v, using equation 1 is plotted in **Fig. 4** for k=0.6 with $f_c^{'}$ = 30 MPa. Also plotted in **Fig. 4** are the crack widths for varying values of clamping and shear stresses based on equations 5 and 6 and assuming a maximum aggregate diameter, a_{agg}, of 10 mm. As mentioned previously, it is felt that

comparing these two models is reasonable as they are both the result of regression analysis using similar data from push-off tests. From **Fig. 4** it can be seen that within a band of crack widths between 0.5 and 0.7 mm, the approaches appear to give consistent results except for very low levels of clamping stress and for clamping stresses above 5 MPa (which is considerably higher than the clamping stresses provided by the straps in the experimental studies). This indicates that for a given $f_c^{'}$ (in MPa) and a_{agg}, one could assume the crack width to be constant without a significant loss of accuracy. For example, for a_{agg} = 10 mm, the aggregate size used in the current work, this relationship was plotted for a variety of concrete strengths and the following approximation was developed:

$$w = \frac{15.5}{f_c^{'}} + 0.03 \tag{10}$$

Although not presented here, further expressions can be developed to reflect the dependency on a_{agg}. The crack width calculated using equation 10 is oriented perpendicular to the direction of the crack but can be resolved to find the associated opening in the vertical direction. Since the prestressed CFRP straps are not bonded to the surface of the beam, the resulting additional strain in the strap due to cracking can therefore be calculated using equation (11).

$$\varepsilon_{cr} = \frac{w}{h_{FRP} \cos\theta} \tag{11}$$

where h_{FRP} can be taken as the height of the strap between the strap supports.

Shear and Flexural Capacity Solution Procedures

To determine the shear capacity of the beam, it is necessary to iterate through the possible crack planes until a minimum solution is determined. In a region of constant shear, for the ‘smeared’ model only the crack angles need to be varied as the same ‘smeared’ reinforcement acts throughout the span. Although this approach may initially seem

complicated, it is based on geometric and material parameters that should be available to the designer. Through the use of a spreadsheet, the minimum value of V_n can be determined quite expediently and the solution procedure is summarised in **Fig 5**.

In addition to finding the minimum value of the shear force carrying capacity, V_n, there are two additional considerations based on the force balance shown in **Fig 2(a)** that need to be discussed. First of all, equation 7 was derived without the need to consider moment equilibrium. This is a useful simplification but one repercussion is that there is then no requirement to calculate the location of the resultant *R* to obtain the shear capacity. However this means that the location of the resultant may not occur within the section thus invalidating the solution without the designer realizing. It was therefore important to conduct a check here to confirm that the location of *R* remained plausible to ensure the solution and proposed model are reasonable (e.g. *R* should lie within the half of the cross section that is in compression for simply supported beams). This was done by taking moments about a point on the critical crack plane, in this case at the location of the force *T*, once the optimum solution for V_n had been determined as the angle of the crack plane was known. When taking moments with the discrete model the exact location of each transverse reinforcement element was known whilst in the smeared approach it was easiest to 'lump' the traverse reinforcement force at the centre of the critical plane. The resultant force, *R*, was located for each specimen in this study was found to lie within the section in all cases, suggesting that the current approach is feasible. Designers wishing to ensure that the resultant force falls within the section under consideration are directed towards the original work by Loov (1998) where the full set of equations required to do this are presented.

A further point of note is that in the calculations an optimum value of the force in the longitudinal reinforcement, *T*, was used with the maximum value being equal to the force required to yield the reinforcement. A simplification proposed by Loov that was referred to earlier. However, as the relationship between *S* and *R* is fixed, then for a given crack angle, only changes in the force *T* in the longitudinal reinforcement will have a direct influence on the clamping force *R*. A possible enhancement to the model would be to

have the clamping force R be dependant on the force in the transverse reinforcement as well as the force in the longitudinal reinforcement. However, there appears to be no simple way to incorporate possible interactions as a result of an increased clamping force due to the strap strains without developing further equations, such as consideration of moment equilibrium to calculate T directly, which would also require further iterations. Since, as will be demonstrated later, using the optimum value of T appears to result in reasonable estimates of shear capacity, it was felt that adding another level of iterations would make this model less useful for design with no great improvement in accuracy.

In the absence of a flexural moment calculation in the shear friction approach, the flexural capacity of the reinforced concrete beam needs to be calculated using either code equations or analysis software. In the results presented here, an analysis package called Response2000 (Bentz and Collins 2000) was used to obtain the flexural capacity of each specimen.

Experimental Database

The predictive method was benchmarked against an experimental database which includes unstrengthened and CFRP strap-strengthened rectangular, T- and deep beams. So while there is typically only a single beam tested for each combination of parameters, the database still represents a broad range of parameters.

Rectangular Specimens

A series of tests on rectangular beams was undertaken by Kesse and Lees (2007). The main variables examined in the experimental program were the strap spacing, s_{FRP}, number of CFRP strap loops and initial prestress in the straps. The main test parameters including the rupture strength of the strap f_{uCFRP} can be found in **Table 1**. The specimen cross-section is illustrated in **Fig. 6(a)** and the transverse reinforcing layout and overall test dimensions are given in **Fig. 6(b)**. The specimens were tested as cantilevers to more

effectively isolate the critical shear span. The longitudinal reinforcement ratio for all these specimens was 2.66%. The specimens were designed so that the difference between the unretrofitted control specimen shear capacity and flexural capacity was approximately 85% to better gauge the effect of adding the CFRP straps. Each of the specimens was tested to failure by increasing the applied load at the end of the cantilever using a hydraulic jack. Details of the experimental test set-up, CFRP strap installation technique and testing procedure can be found in Kesse and Lees (2007).

Whereas the unstrengthened control beam failed in shear, Kesse and Lees found that if the strap spacing was smaller than the effective depth of the beam and a sufficient number of strap loops were used, equivalent strengthened beams failed in flexure. In addition, for the particular specimen geometry tested, the effect of CFRP strap prestress on the overall beam capacity appeared not to be very significant.

T-beam Specimens

T-beam tests by Kesse *et al.* (2001) were combined with selected results from Hoult (2005) to form the T-beam database considered here. Kesse *et al.* (2001) tested two T-beams. The first was a control specimen and the second was retrofitted with the CFRP straps. Three specimens tested by Hoult (2005), consisting of one control and two retrofitted specimens which, with the exception of the concrete strength, had nominally identical material and geometric properties to the specimens tested by Kesse *et al*. are also included. The cross-section and reinforcement layout for all five specimens is given in **Fig. 7(a)**. The transverse reinforcement layout and overall testing dimensions are given in **Fig. 7(b)**. The key testing parameters are presented in **Table 2**. The longitudinal reinforcement ratio for all T-specimens was 4.36%. The specimens were designed so that the difference between the unretrofitted control specimen shear capacity and flexural capacity was approximately 50% so that, as with the rectangular specimens, the effect of the CFRP straps could be distinguished more clearly. The beams were tested in four-point bending using a gradually increasing load applied by two hydraulic jacks. Details of the

experimental test set-up, CFRP strap installation technique and testing procedure can be found in Hoult (2005).

In the specimens tested by Kesse *et al.* the straps were installed through grooves in the flange and supported by metal pads on the top and bottom of the specimen as illustrated in **Fig. 1**. In the specimens tested by Hoult the straps were instead installed so that access to the top surface of the beam was not required as illustrated in **Fig. 7(a)**. The top cover to the straps, c_{FRPT}, in these specimens and as used in the model was 20 mm. In all cases, considerable increases in capacity were achieved with the strengthening system.

Deep Beam Specimens

A series of five deep beam specimens was tested by Stenger (2000). The cross section of each specimen is given in **Fig. 8(a)** while the layout of the transverse reinforcement is given in **Fig. 8(b)**. The key testing parameters are given in **Table 3**. The longitudinal reinforcement ratio was 1.95%. As was the case for the other test series, the specimens were designed so that the difference between the unretrofitted specimen shear capacity and the retrofitted specimen capacity was significant to determine the effect of the CFRP straps. By displacing one end of the specimen relative to the other an increasing shear force that was constant along the length of the specimen was applied up to failure. Details of the experimental test set-up, CFRP strap installation technique and testing procedure can be found in Stenger (2000). Specimens ST1, ST4 and ST5, which had strap prestress levels of 56% of the ultimate strap capacity, saw significant increases in their load carrying capacity versus the control specimen, ST2. Specimen ST3, with a prestress of only 4% of the ultimate strap capacity, failed at a load very close to that of the control specimen. Unlike Kesse and Lees (2007), Stenger found that the amount of prestress in the CFRP straps had a considerable impact on the overall specimen capacity suggesting that the specimen depth is an important factor.

Smeared Model Verification

As discussed, both a 'smeared' and a 'discrete' formulation have been developed. In the following, the 'smeared' results will be presented to determine the ability to predict the unstrengthened and strengthened capacity of the beams and to compare the influence of the clamping force. The limitations of this 'smeared' assumption will then be explored by comparing selected results with those obtained with the 'discrete' approach.

Table 4 gives the experimental capacity for each specimen (V_{exp}), the predicted capacity from the smeared model (V_{pred}) and the ratio V_{pred} / V_{exp} for that model. **Table 4** also provides the experimental failure mode (FM_{exp}), the predicted failure mode (FM_{pred}) for the 'smeared' model and the predicted crack angles (θ_{pred}) where this is the crack angle in the web for the T-beam specimens. Finally, the experimental strap strain at failure (ε_{exp} @ failure), the experimental strap strain at predicted failure (ε_{exp} @ pred failure), the predicted strap strain using the 'smeared' model ($\varepsilon_{prestress} + \varepsilon_{cr}$) and the predicted maximum strap strain at failure (ε_{max}) are also indicated.

Load Carrying Capacity Predictions

Overall the model predicted the maximum load carrying capacity of the specimens well with a mean V_{pred} / V_{exp} ratio of 0.94 and a Coefficient of Variation (C.OV.) of 0.08, which suggests the model is both accurate and precise.

Unstrengthened control beam predictions

The capacities of the unstrengthened control beams were predicted well with the caveat that the strength of the rectangular control beam B2-ns-nl was overestimated and the capacity of deep beam ST2 was underestimated. For specimen B2-ns-nl, this appears to have been due to the use of the 'smeared' assumption as will be discussed later. The accurate prediction of the unstrengthened T-beam capacities is encouraging, as many existing code models tend to be conservative for T-beams (Zoeheary *et al.* 1998).

Strengthened beam predictions

The mode of failure (shear versus flexure) was generally well-predicted. However, all the shear failures were predicted to be concrete shear failures and the rupturing of the CFRP straps was predicted with limited success for the 'smeared' model. The strap strains presented in **Table 4** indicate that the experimental strap strains at failure (ε_{exp} @ failure) for the specimens where strap rupture occurred are generally underestimated by the model. This is believed to be due to the fact that the strap strains given by the model are based on average shear stresses and are therefore average strains. The experimental strains, on the other hand, are from straps that could potentially cross the crack at any point along its length. If the straps crossed the crack at the location of maximum width, for example, the measured strains would be higher than the predicted strains. To better reflect this behaviour, an equation for the maximum predicted strap strain is developed by assuming that the crack width varies linearly from a minimum of 0 at the tip of the crack to a maximum value of $2w$ at the end of a crack that extends over the full height of the section. This is a simplification as shear cracks in beams have varying widths as well as varying angles along their length and do not typically extend over the full height of the section but it will allow an upper limit to be calculated. The resulting maximum predicted strain, ε_{max}, in a strap using the 'smeared' model can be found from:

$$\varepsilon_{max} = \varepsilon_{prestress} + 2\varepsilon_{cr} \tag{12}$$

The resulting ε_{max} calculated for each specimen has been included in **Table 4** and generally provides a reasonable upper limit of the strap strain with the notable exception of B12-2s-10l-5p. In specimen B12-2s-10l-5p, a beam with a low level of prestress, the experimental crack angles were similar to those predicted by the model and, although not presented here, the predicted failure load using the 'discrete' model was similar to that using the 'smeared' model. Yet the predicted strap strains for the specimen were much lower than the experimental strains at failure. This result requires further examination as slender specimens with low levels of prestress potentially have fundamentally different behaviour. In this case it is possible that as the cracks opened the concrete contribution

decreased but the additional strain in the CFRP strap caused by the wider cracks allowed for the shear force to be transferred into the straps until they too ruptured. However, the model will give conservative load carrying capacity predictions as it uses the strap strains that are developed when the concrete contribution is a maximum and thus any additional strap strains after this point are ignored. This is illustrated by comparing the experimental strap strains at the predicted failure load of 83 kN to those calculated by the model (an experimental strain, ε_{exp} @ pred failure, = 0.0040 versus a predicted strain, ε_{max}, of approximately 0.0043). It was only after an applied load of approximately 83kN that the strap strains began to increase dramatically for this specimen.

The model was also able to reflect the beneficial effects of prestress. For example, the difference in the predicted capacities of ST3 (with a prestress of 4%) versus ST4 and ST5 with 56% prestress were consistent with the experimental observations. The increase in crack angle due to increasing prestressing force was also apparent with the predicted failure angle of 42° being much steeper for ST4 (and ST5) than the 31° angle predicted for ST3. By increasing the crack angle the prestress in the straps indirectly increases the clamping stress by increasing the value of *T*, which as mentioned before is a function of the crack angle. The predicted crack angles were generally consistent with the experimental crack angles with the exception of B9-1s-10l-50p. This incorrect prediction is believed to be due to the smearing assumption and will be discussed in more detail in the next section.

Discrete versus Smeared Strap Model

In the ‘smeared’ model the exact location of the reinforcement relative to the failure plane is irrelevant. In the ‘discrete’ model, the location of the reinforcement will influence the location of the critical failure plane. In general the ‘smeared’ model is much easier to use in a region of constant shear as it only requires the designer to vary the crack angles, which as outlined earlier can be done quite easily with a spreadsheet. The ‘discrete’ approach on the other hand requires the designer to iterate through a number of different crack plane angles and locations, which if the internal steel transverse

reinforcement spacing and CFRP strap spacing are different, as was the case in all three experimental studies, can be quite time consuming. There is also a greater potential for error if the designer fails to check all the potential combinations and misses the critical one. As such the focus of this paper has been on the 'smeared' approach as it seems preferrable in terms of efficiency and simplicity. Indeed if the internal and external reinforcement spacing to effective depth ratios are small, then the differences in the predicted capacities using the 'smeared' versus the 'discrete' approach are not expected to be great. However, if these ratios are large, the smearing assumption may no longer be valid and it is necessary to determine the location of the critical failure plane to accurately determine the beam's capacity. This effect is compounded if the contribution of an individual transverse reinforcement element is also high (i.e. high transverse reinforcing ratios or high strap prestress) since the deviation of the 'discrete' from the 'smeared' behaviour is made more significant by the large increases in capacity at the discrete locations of each reinforcing element.

Fig. 9(a) gives the results of the maximum shear force carrying capacity versus the crack angle (θ) for the 'smeared' and 'discrete' models for two specimens: B2-ns-nl, an unstrengthened rectangular section and B10-2s-5l-50p, a strengthened rectangular specimen with two straps of relatively low stiffness. It can be seen in **Fig. 9(a)** that there is a step in the capacity each time an internal steel stirrup or external CFRP strap is crossed. The strap locations are represented as discrete changes in capacity although in practice there will be a region of influence around the strap support pads. Also presented in **Fig. 9(a)** is a line indicating the crack angle at which the force, T, in the longitudinal reinforcement from Loov's (1998) model exceeds the yield strength of the reinforcement. Since the clamping force is a function of T, this limits the amount of force that can be transferred through shear friction for crack angles greater than this value. However, as can be seen from **Fig. 9(a)**, the angles at which this occurs are well above those observed in the experiments.

Examining **Fig**. **9(a)** one can see that the 'smeared' model provides a slightly unconservative estimate of the control specimen capacity whereas using the 'discrete'

model provides an accurate prediction of not only the specimen capacity but also the failure crack angle. It is perhaps not surprising that a discrete approach is more effective for predicting the capacity of specimen B2-ns-nl since it had a small transverse reinforcement ratio suggesting that the assumption of smeared reinforcement could be inappropriate. In the case of specimen B10-2s-5l-50p the 'discrete' approach again provides an accurate prediction of the failure load and crack angle (see **Fig. 9(b))**. Thus it seems that for some specimens where the smeared reinforcement assumption is inappropriate it is possible to achieve better estimates of the specimen capacity by considering the transverse reinforcement as discrete elements. In general though, well detailed CFRP strap retrofitting systems with appropriate levels of strap stiffness, spacing and prestress seem to be predicted effectively by the simpler 'smeared' model. However, a larger database of specimens will be required before the limits of the 'smeared' model can be known with certainty and thus applied to design.

The requirements set out for this model were to effectively account for the unbonded and prestressed nature of the CFRP straps, to attempt to account for the clamping effects provided by the straps, to establish when strap rupture governs, and to determine if a smeared reinforcement assumption was reasonable. By determining the crack widths at the level of maximum shear friction capacity, the unbonded and prestressed nature of the straps could be addressed by calculating the strain due to prestress and cracking over the full height of the strap. An upper limit could then be calculated for this strap strain which in most cases seems to accurately predict if rupture will occur. The effects of clamping provided by the prestress were reflected indirectly by the increase in the crack angle which then increased the clamping provided by the longitudinal reinforcement. The best illustration of this effect was provided by the deep beam predictions. Finally the assumption of smeared reinforcement behaviour appeared to be reasonable for specimens with sufficient levels of transverse reinforcement as long as the spacing was controlled. This result correlates well with typical design code approaches that also specify minimum transverse reinforcement areas and maximum spacing limits. Overall the model seems to account for all of the critical variables resulting in fairly accurate predictions of specimen behaviour.

Conclusions

A shear friction based approach incorporating crack widths has been used to develop two models to predict the capacity of beams with and without CFRP strap retrofitting. One of these models considered the transverse reinforcement elements, both the steel stirrups and CFRP straps, to be smeared along the length of the beam. A second model considered the transverse reinforcement to be a series of discrete elements where the maximum shear strength was calculated by varying the angle of the crack plane. Both of these approaches were found to be accurate in terms of predicting the capacity of the specimens in the test database composed of rectangular, T- and deep beams. The ‘smeared’ approach was the easier to employ numerically requiring only the crack angle to be varied to find the optimum solution. This method produced accurate estimates in terms of specimen capacity and can also produce a realistic upper limit on the strap strains for most specimens. For specimens where the transverse reinforcement cannot reasonably be assumed to be smeared (e.g. the spacing of the elements is too large), the ‘discrete’ model can be used to offer better estimates of specimen capacity. Though the models were found to work well in most cases, the capacity of a rectangular specimen with low initial prestress was not predicted well. This result indicates the need for further testing in order to validate the models but the results to date suggest that the models are both accurate and precise for a variety of specimen types.

Acknowledgements

The authors wish to thank EMPA for their generous support and Dr G. Kesse for his help and advice. The first author wishes to thank the Cambridge Commonwealth Trust and Universities UK for their financial support.

References

Bentz, E. and Collins, M.P. (2000). *Response-2000 Reinforced Concrete Sectional Analysis using the Modified Compression Field Theory, Version 1.0.5*, Software Package, Toronto.

Berset, J.-D. (1992). *Strengthening of Reinforced Concrete Beams for Shear Using FRP Composites*, MSc Thesis, Massachusetts Institute of Technology, Cambridge, Mass.

Deniaud, C. and Cheng, J.J.R. (2001). "Shear Bevaviour of Reinforced Concrete T-Beams with Externally Bonded Fiber-Reinforced Polymer Sheets." ACI Structural Journal, 98 (3), 386-394.

Deniaud, C. and Cheng, J.J.R. (2003). "Reinforced Concrete T-Beams Strengthened in Shear with Fiber Reinforced Polymer Sheets." ASCE Journal of Composites for Construction, 7 (4), 302-310.

Duthinh, D. (1999). "Sensitivity of shear strength of reinforced concrete and prestressed concrete beams to shear friction and concrete softening according to modified compression field theory." ACI Structural Journal, 96(4), 495-508.

Hofbeck, J.A., Ibrahim, I.O. and Mattock, A.H. (1969). "Shear Transfer in Reinforced Concrete," Journal of the ACI, 66(2), 119-128.

Hoult, N.A. (2005). "Retrofitting of Reinforced Concrete Beams with CFRP Straps to Enhance Shear Capacity." PhD Thesis, University of Cambridge, Cambridge, UK.

Hoult, N.A. and Lees, J.M. (2007). "Approaches to Modeling an Unbonded CFRP Strap Shear Strengthening System for RC Beams." Proc. of the Eighth International Symposium on Fiber Reinforced Polymer for Reinforced Concrete Structures, Patras, Greece, 10pp.

Hoult, N.A. and Lees, J.M. "Efficient CFRP Strap Configurations for the Shear Strengthening of Reinforced Concrete T-beams." ASCE Journal of Composites for Construction, *in press*.

Kesse, G., Chan, C. and Lees, J.M. (2001). "Non-linear Finite Element Analysis of RC Beams Prestressed with CFRP Straps." Proc. of the Fifth International Symposium on Fiber Reinforced Polymer for Reinforced Concrete Structures, Cambridge, UK, Volume 1, pp 281-290.

Kesse, G. and Lees, J. M. (2007). "Experimental Behavior of Reinforced Concrete Beams Strengthened with Prestressed CFRP Shear Straps," Jour. of Composites for Construction, 11 (4), 373-383.

Khalifa, A., Gold, W.J., Nanni, A. and Abdel Aziz, M.I. (1998). “Contribution of Externally Bonded FRP to Shear Capacity of RC Flexural Members.” Jour. of Composites for Construction, 2 (4), 195-202.

Kumaraguru, P. (1992). “Strength of dapped-end beams.” M.Sc. thesis, The University of Calgary, Calgary, Alberta.

Loov, R.E. (1998). “Review of A23.3-94 simplified method of shear design and comparison with results using shear friction.” Canadian Journal of Civil Engineering, 25 (3), 437-450.

Loov, R. and Peng, L. (1998). “The Influence of Concrete Strength on Shear Friction based Design of Reinforced Concrete Beams.” Proc. of the International Conference on HPHSC, Perth, Australia, 505-519.

Mattock, A.H. and Hawkins, N.M. (1972). “Shear Transfer in Reinforced Concrete – Recent Research.” PCI Journal, 17 (2), 55-75.

Melo, G.S., Araujo, A.S. and Nagato, Y. (2003). “Strengthening of RC T Beams in Shear with Carbon Sheet Laminates (CFRP).” Proc. of the Sixth International Symposium on FRP Reinforcement for Concrete Structures, Singapore, Vol. 1, 477-486.

Stenger, F. (2000). “Tragverhalten von Stahlbetonscheiben mit vorgespannter externer Kohlenstofffaser-Schubbewehrung.“ Doctor of Technical Sciences Thesis, Swiss Federal Institute of Technology (ETH), Zurich, 155pp.

Tozser, O. and Loov, R. (1999). “Shear Design of Prestressed Beams using Shear Friction.” Proc. of the Annual Conference of the Canadian Society for Civil Engineering, CSCE, Regina, Manitoba, 195-204.

Vecchio, F.J. and Collins, M.P. (1986). “The Modified Compression-Field Theory for Reinforced Concrete Elements Subjected to Shear.” ACI Journal, 83 (2), 219-231.

Walraven, J.C. (1981). “Fundamental Analysis of Aggregate Interlock.” ASCE Journal of the Structural Division, 107 (ST11), 2245-2270.

Walraven, J.C., Frenay, J. and Pruijssers, A. (1987). “Influence of Concrete Strength and Load History on the Shear Friction Capacity of Concrete Members,” PCI Journal, 32 (1), 66-84.

Winistoerfer, A.U. (1999). “Development of non-laminated advanced composite straps for civil engineering applications.” PhD Thesis, University of Warwick, Coventry, UK.

Zoeheary, A.A., Farahat, A.M. and El. Degwy, W.M. (1998), “Behaviour of Reinforced Concrete T-Beams.” Journal of Engineering and Applied Science, 45 (4), 513-531.

Table 1 – Rectangular Specimen Parameters

Specimen	s_{FRP} (mm)	No. of Loops	Strap Area (mm^2)	E_{FRP} (MPa)	f_{uCFRP} (MPa) (% prestress)	f_{yv} (MPa)	f_{cu} / f'_c (MPa)
B2-ns-nl	NA	0	0	130000	1430 (0)	400	62.3 / 49.8
B5-2s-10l-50p	230	10	38.4	130000	1430 (50)	400	49.7 / 39.8
B6-1s-5l-50p	690	5	19.2	130000	1430 (50)	400	47.9 / 38.3
B7-1s-5l-50p*	690	5	19.2	130000	1430 (50)	400	43.5 / 34.8
B8-2s-10l-50p*	230	10	38.4	130000	1430 (50)	400	44.0 / 35.2
B9-1s-10l-50p	690	10	38.4	130000	1430 (50)	400	41.0 / 32.8
B10-2s-5l-50p	230	5	19.2	130000	1430 (50)	400	43.5 / 34.8
B11-2s-10l-25p	230	10	38.4	130000	1430 (25)	400	45.9 / 36.7
B12-2s-10l-5p	230	10	38.4	130000	1430 (5)	400	45.9 / 36.7

* specimens were preloaded to 34kN before the retrofit was installed

Table 2 – T-beam Specimen Properties

Specimen	s_{FRP} (mm)	No. of Loops	Strap Area (mm^2)	E_{FRP} (MPa)	f_{uCFRP} (MPa) (% prestress)	f_{yv} (MPa)	f_{cu} / f'_c (MPa)
B1/25	0	0	0	NA	NA	578	24.8 / 19.8
B6/30/C/44	250	10	38.4	121000	1536 (25)	578	43.9 / 35.1
B7/30/G/36	200	10	38.4	121000	1536 (25)	578	36.1 / 28.9
Control	0	0	0	NA	NA	380	50 / 40
Retrofit	200	10	38.4	121000	1536 (50)	380	45 / 36

Table 3 – Deep Beam Specimen Properties

Specimen	s_{FRP} (mm)	No. of Loops	Strap Area (mm^2)	E_{FRP} (MPa)	f_{uCFRP} (MPa) (% prestress)	f_{yv} (MPa)	f_{cu} / f'_c (MPa)
ST1	500	25	96	130000	1200 (56)	605	36 / 28.8
ST2	NA	0	0	NA	NA	605	36.8 / 29.4
ST3	500	25	96	130000	1200 (4)	605	39.2 / 31.4
ST4**	500	25	96	130000	1200 (56)	605	37.6 / 30.1
ST5***	500	25	96	130000	1200 (56)	605	39.1 / 31.3

** specimen were preloaded to 350kN before the retrofit was installed

*** specimen was loaded up to 67% of the maximum shear capacity in one direction then loaded to failure in the opposite direction

Table 4 – Beam Modelling Results

Specimen	V_{exp} (kN)	V_{pred} (kN)	$\frac{V_{pred}}{V_{exp}}$	FM_{exp}	FM_{pred}	θ_{pred} (°)	ε_{exp} @ failure	ε_{exp} @ pred failure	$\varepsilon_{prestress} + \varepsilon_{cr}$	ε_{max}
B2-ns-nl	52	56.1	1.08	S.C.	S.C.	23	-	-	-	-
B5-2s-10l-50p	97.7	88.4	0.90	Flexure	Flexure	39	0.0063	0.0060	0.0075	0.0095
B6-1s-5l-50p	81.2	70.3	0.87	S.S.	S.C.	27	0.0081	0.0062	0.0072	0.0090
B7-1s-5l-50p*	75.5	68.9	0.91	S.S.	S.C.	28	N.A.	N.A.	0.0074	0.0093
B8-2s-10l-50p*	96.1	89.9	0.94	Flexure	Flexure	41	N.A.	N.A.	0.0078	0.0100
B9-1s-10l-50p	87.6	80.0	0.91	S.C.	S.C.	32	0.0068	0.0061	0.0076	0.0098
B10-2s-5l-50p	79.8	87.0	1.09	S.S.	Flexure	35	0.0108	-	0.0076	0.0096
B11-2s-10l-25p	97	87.0	0.90	Flexure	Flexure	35	0.0072	0.0054	0.0047	0.0067
B12-2s-10l-5p	89	83.0	0.93	S.S.	S.C.	30	0.0111	0.0040	0.0024	0.0043
Control	100	99.4	0.99	S.C.	S.C.	28	-		-	-
Retrofit	148	143.0	0.97	Flexure	Flexure	44	0.0090		0.0071	0.0091
B1/25	88.2	87.8	1.00	S.C.	S.C.	42	-		-	-
B6/30/C/44	140.9	136.0	0.97	S.C.	Flexure	41	0.0075	0.0066	0.0047	0.0069
B7/30/G/36	134.7	132.0	0.98	Flexure	Flexure	44	0.0063	0.0061	0.0053	0.0081
ST1	703	600	0.85	Shear	S.C.	43	N.A.	N.A.	0.0058	0.0064
ST2	465	371	0.80	Shear	S.C.	29	-		-	-
ST3	479	429	0.90	Shear	S.C.	31	N.A.	N.A.	0.0009	0.0014
ST4**	677	613	0.91	Shear	S.C.	42	N.A.	N.A.	0.0058	0.0064
ST5***	647	624	0.96	Shear	S.C.	42	N.A.	N.A.	0.0057	0.0063
		Mean	0.94							
		COV	0.08							

* specimens were preloaded to 34kN before the retrofit was installed

** specimen were preloaded to 350kN before the retrofit was installed

*** specimen was loaded up to 67% of the maximum shear capacity in one direction then loaded to failure in the opposite direction

S.C. – shear failure in the concrete

S.S. – shear failure due to CFRP strap rupture

N.A. – not available

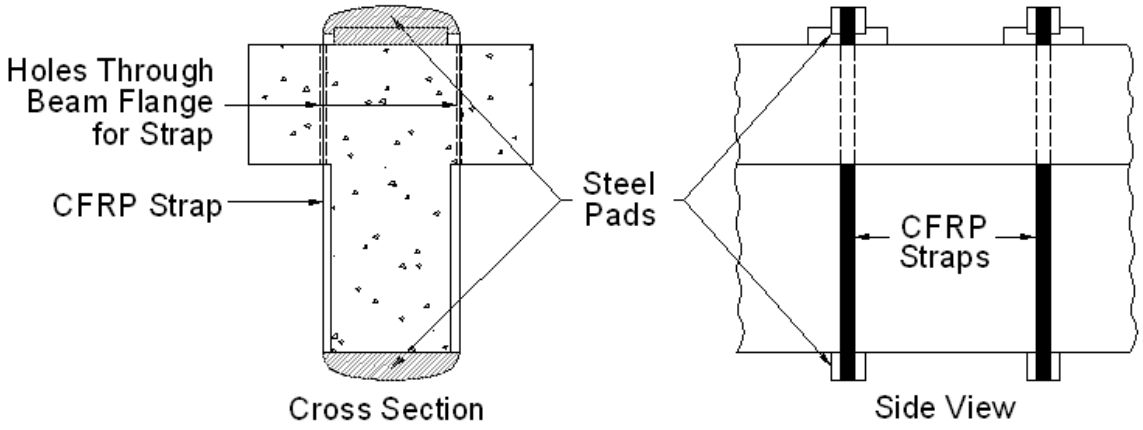

Fig. 1 – CFRP strap configuration

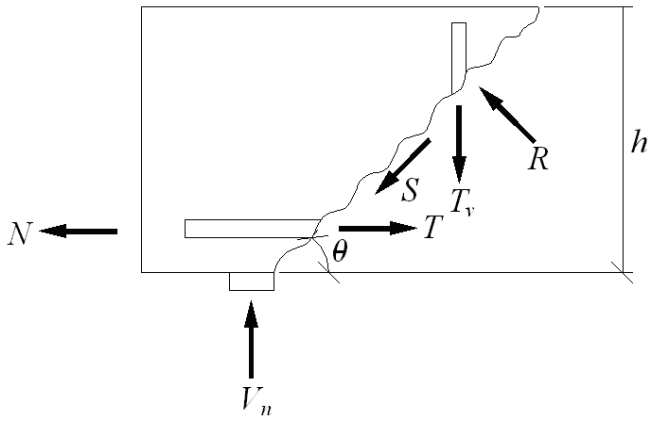

(a)

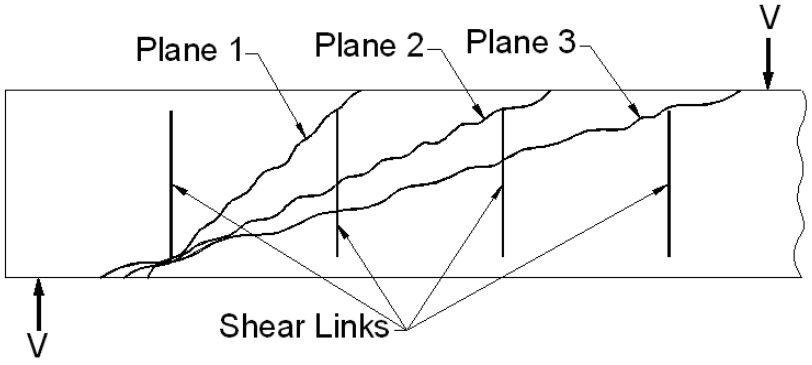

(b)

Fig. 2 – Model as proposed by Loov (1998) (a) Equilibrium across the crack (b) Potential shear planes

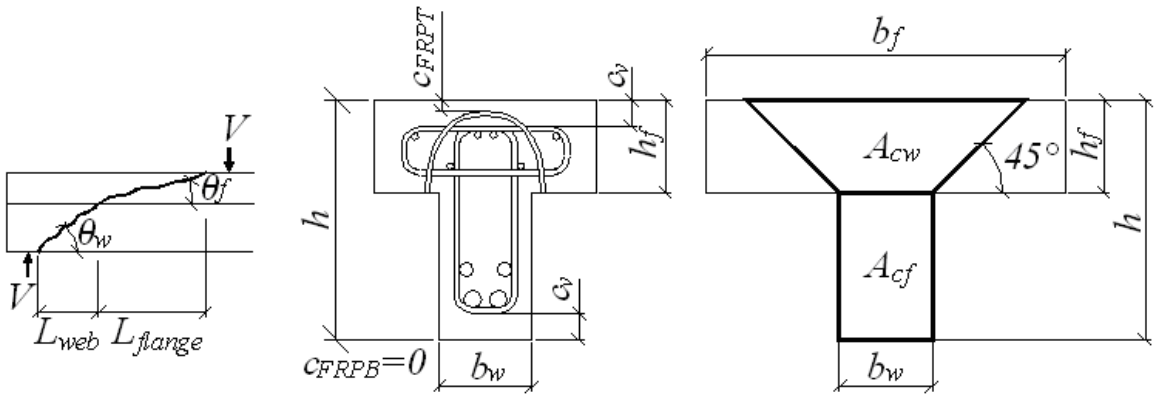

Fig. 3 – Effective areas and dimensions for use with equation (10)

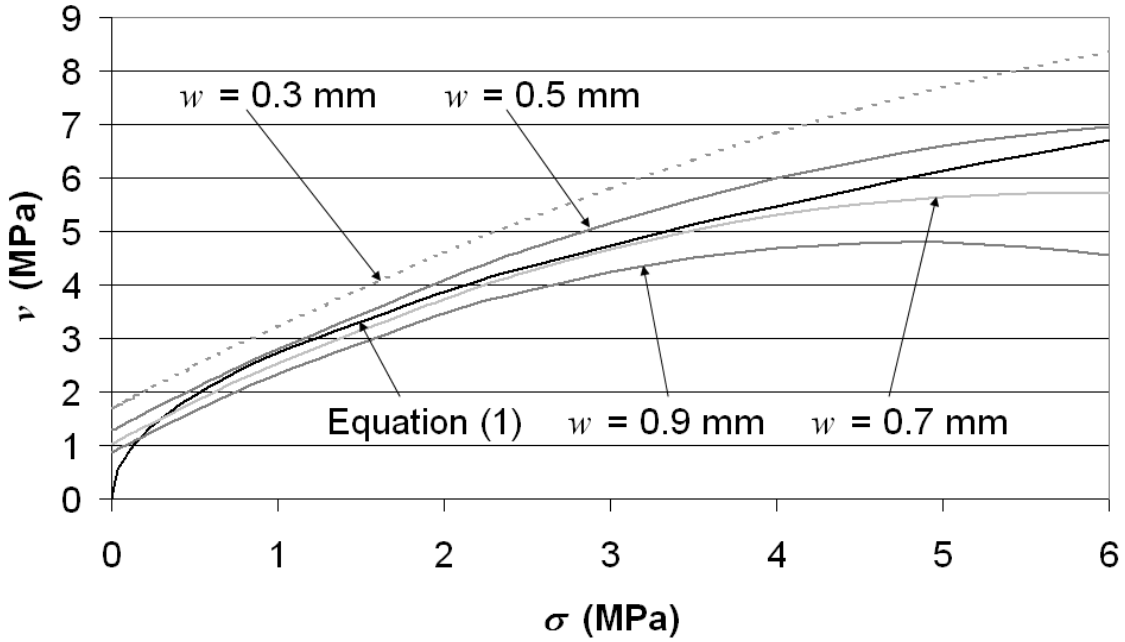

Fig. 4 – Comparison of the Loov (1998) shear friction approach and the Vecchio and Collins (1986) crack width model with f_c' = 30 MPa, a_{agg} = 10 mm

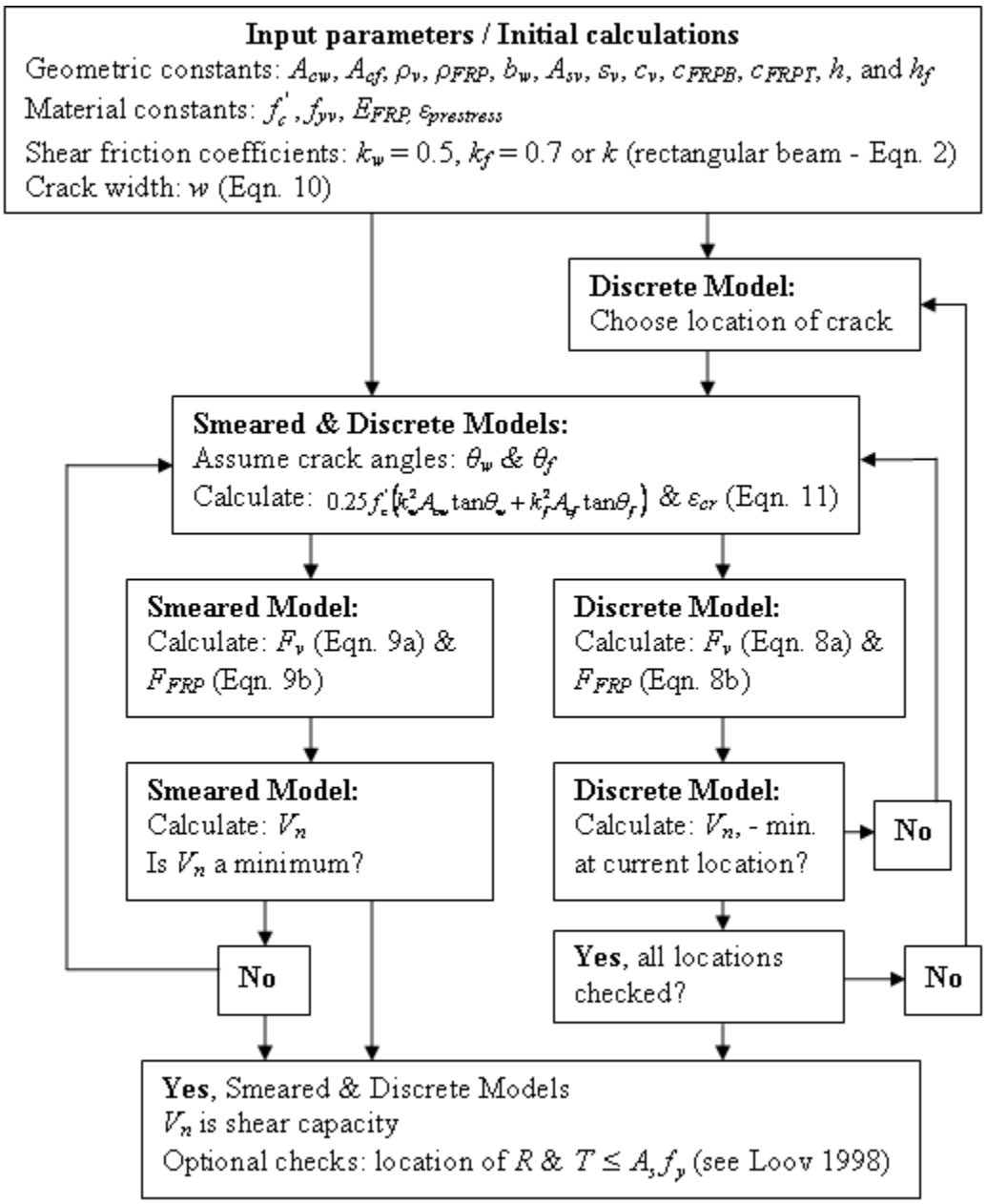

Fig. 5 – Solution procedure for constant shear

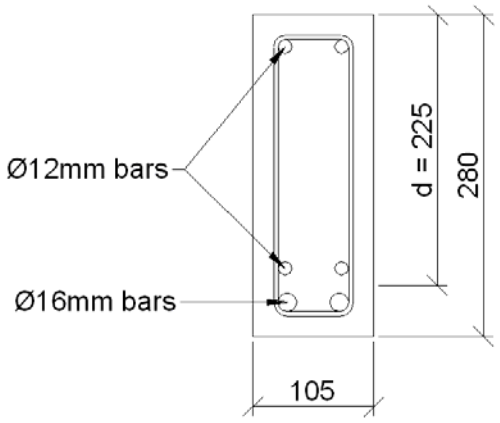

(a)

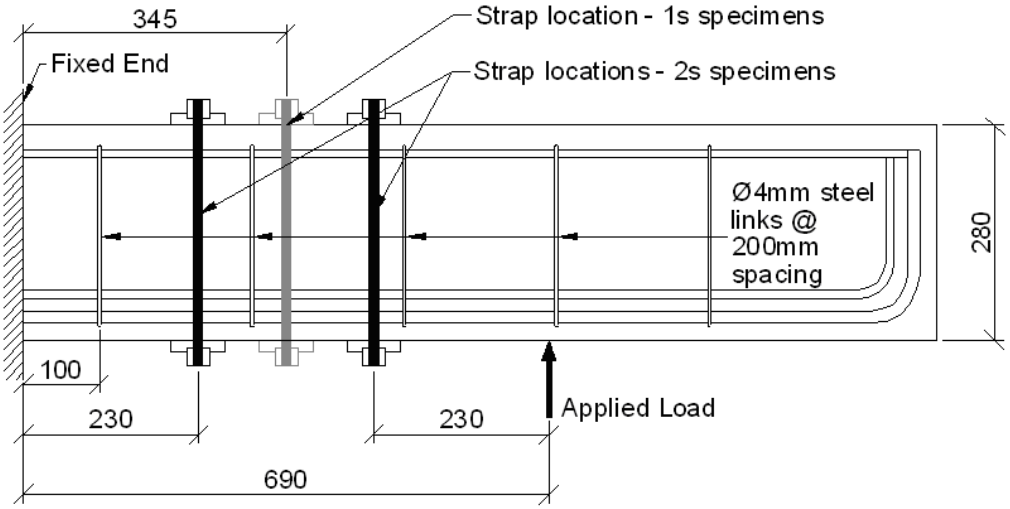

(b)

Fig. 6 – Rectangular specimen layout (a) Cross-section and (b) Transverse layout

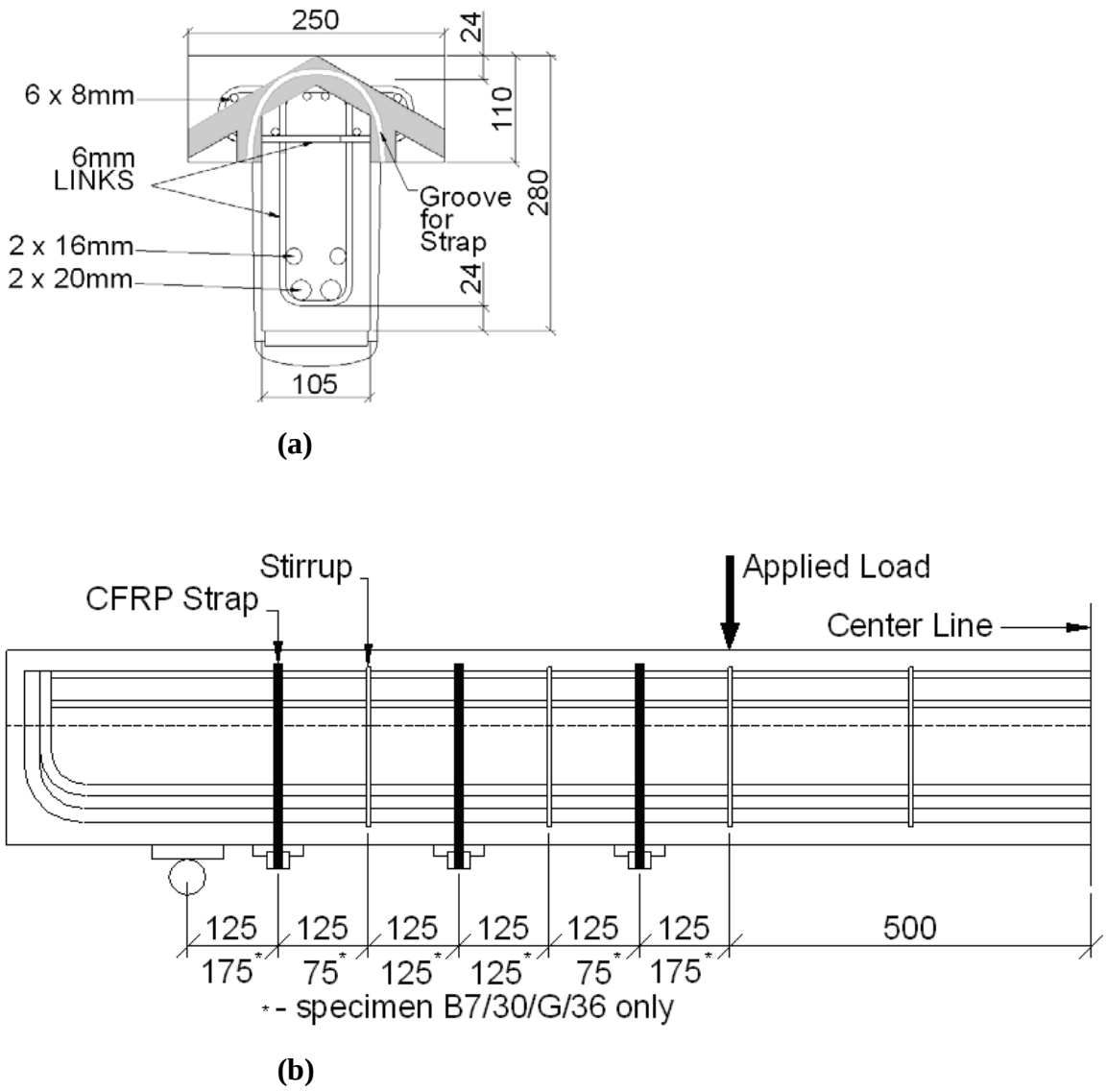

Fig. 7 – T-beam specimen layout (a) Cross-section (b) Transverse layout

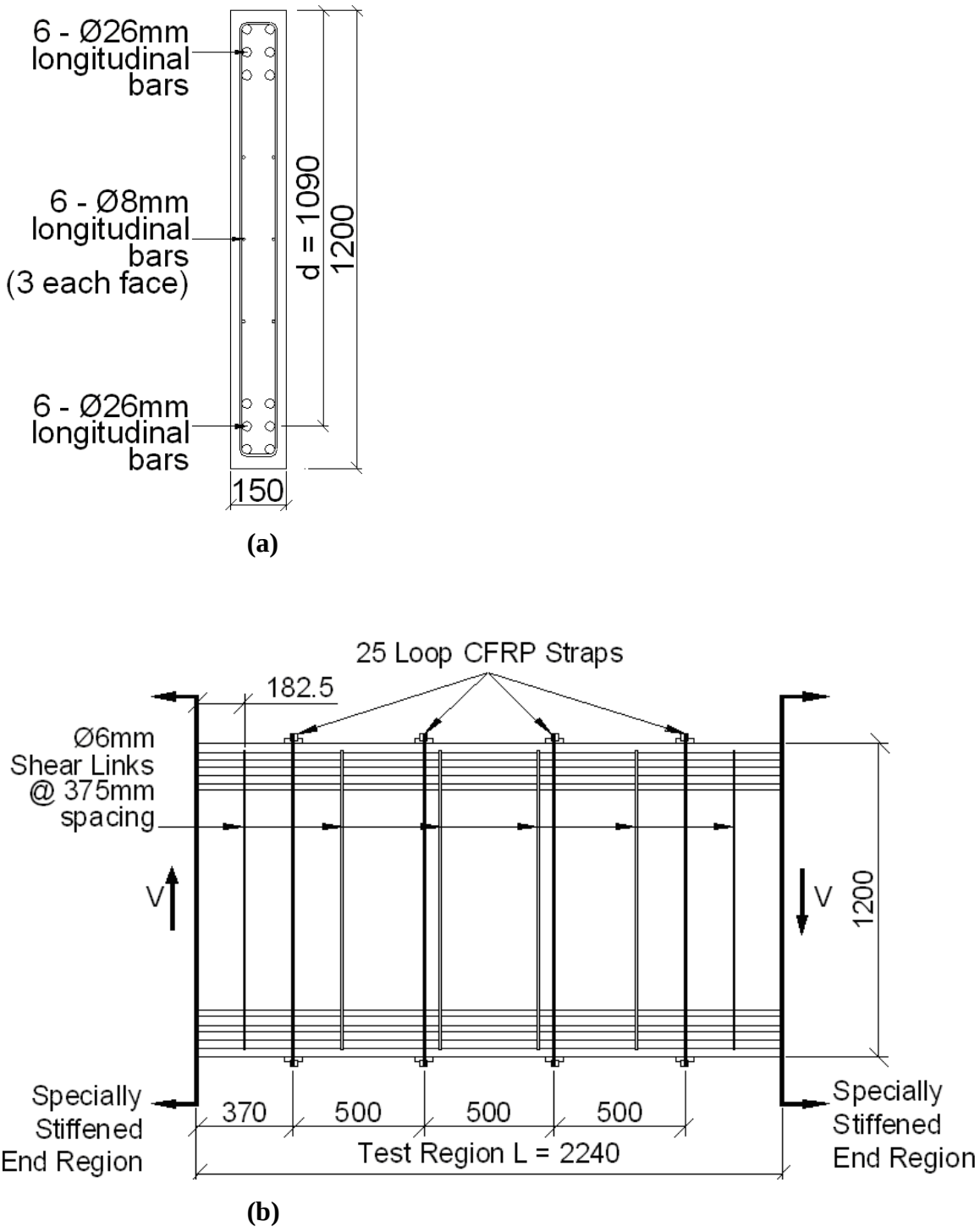

Fig. 8 – Deep beam specimen layout (a) Cross-section (b) Transverse layout

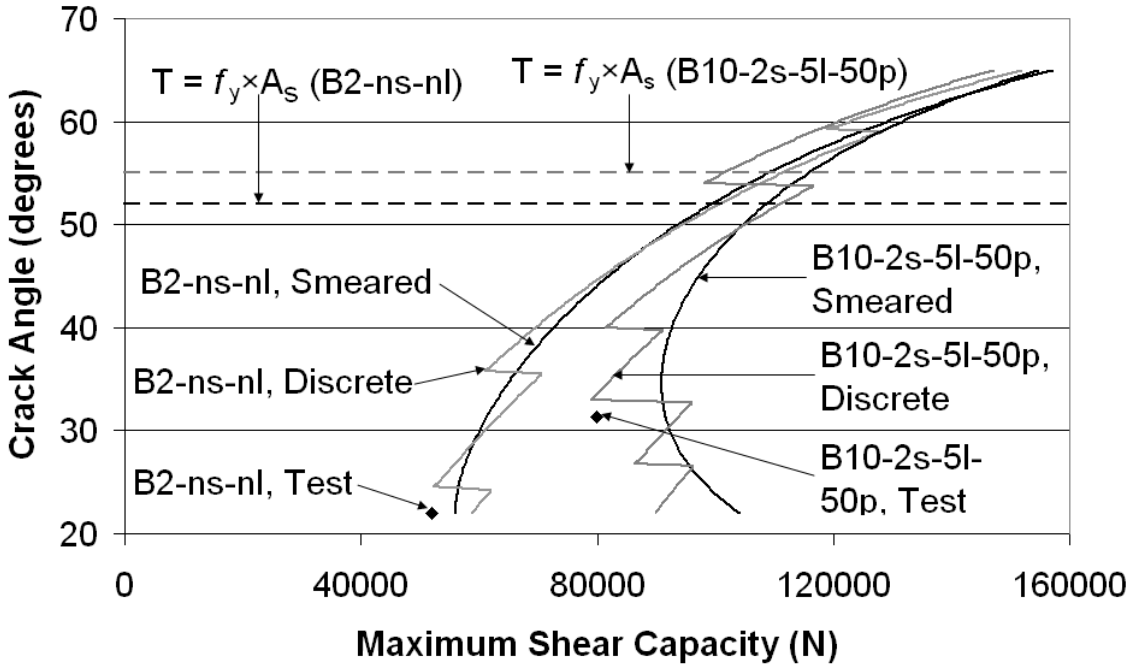

(a)

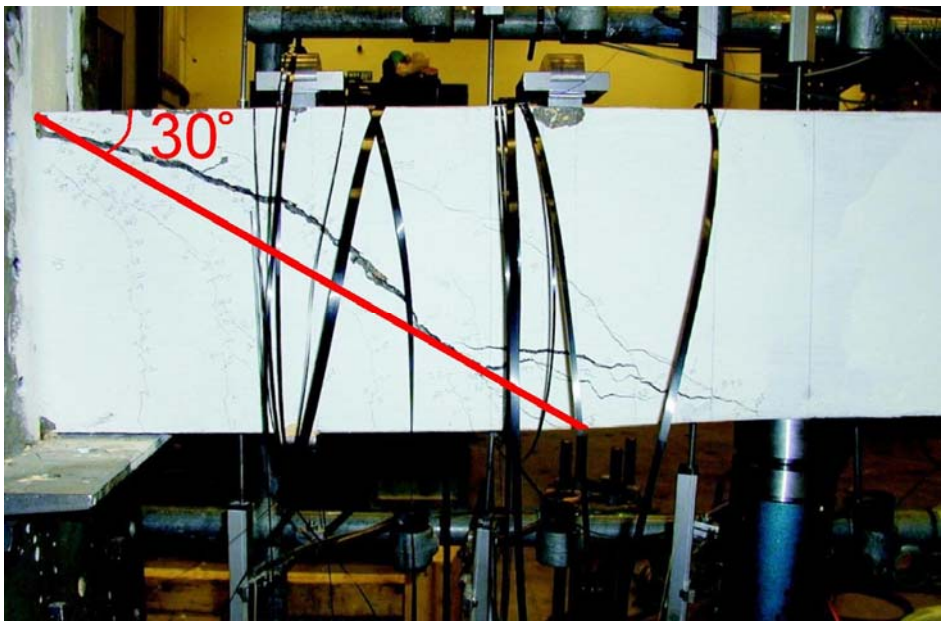

(b)

Fig. 9 – Comparison of Discrete versus Smeared Models (a) Plot of discrete vs. smeared results (b) Specimen B10-2s-5l-50p at failure